Nano Energy 30 (2016) 155–161

Contents lists available at ScienceDirect

Nano Energy

journal homepage: www.elsevier.com/locate/nanoen

Robust design of unearthed single-electrode TENG from three-dimensionally hybridized copper/polydimethylsiloxane film

Meng Zhang[a], Yang Jie[a,b], Xia Cao[a,b,*], Jie Bian[d], Tao Li[a], Ning Wang[d,*], Zhong Lin Wang[a,c,*]

[a] Beijing Institute of Nanoenergy and Nanosystems, Chinese Academy of Sciences, National Center for Nanoscience and Technology (NCNST), Beijing 100083, China
[b] School of Chemistry and Biological Engineering, University of Science and Technology Beijing, Beijing 100069, China
[c] School of Material Science and Engineering, Georgia Institute of Technology, Atlanta, GA 30332-0245, United States
[d] Center for Green Innovation, School of Mathematics and Physics, University of Science and Technology Beijing, Beijing 100069, China

ARTICLE INFO

Keywords:
Cu-PDMS film
Unearthed
Single-electrode mode
Triboelectric nanogenerator
Integrated electrochromic film

ABSTRACT

Developing novel smart materials for the next generation of advanced electronic devices represents a major challenge as well as an exciting opportunity in the direction of integration, miniaturization, and flexibility. Here an unearthed single-electrode triboelectric nanogenerator (TENG) is fabricated from three-dimensionally hybridized copper/polydimethylsiloxane powering films. This robust design simplifies the traditional contact-separation mode so that the as-fabricated single-electrode TENG is simple, stable, waterproof and can be operated without grounding. The output current reaches 1.2 μA cm^{-2} when a pressure as small as 5 N cm^{-2} is applied, which leads to the invention of a pressure sensitive device by integrating with an electrochromic film. The pioneering unearthed single-electrode working modes start up a multifunctional platform for both energy harvesting and self-powered touch sensors.

1. Introduction

Currently electrochemical cells such as Li-ion batteries dominate the market of electrochemical power sources for portable electrical apparatus while the constant expansion of intelligent applications stepped up the demands for much higher energy-density [1,2]. Thus, efficiently miniaturized electrical devices for energy delivery or harvesting with high-performance are urgently needed because they can provide almost inexhaustible power by converting ambient energies into electricity [3]. However, up to now, most of such converters are based on electromagnetic induction effect, which are usually bulky and complex [4–7]. As a result, portable, cost-effective and flexible approaches that can directly harvest mechanical energy for public utilities become the hot favorite.

Triboelectric nanogenerators (TENGs) are a type of electronic devices that can efficiently convert ambient mechanical energy such as human activities, tire rotation, ocean waves and mechanical vibration into electricity via triboelectric and electrostatic induction effects [3,6]. At present, TENGs have been widely used in trace memory systems [8], self-charging cells [9], distress signal emitters [10], self-electroplating technology [11] and self-powered sensors [10,12–19]. The state-of-art TENGs are generally built in contact-separation mode and composed of two electrodes with different surface potentials, which not only demands complicated process and precise operations, but also largely limits the applications in some tough conditions owing to the packaging issues [3,15,20,21]. For self-powered electrochemical system, stable structure, simple fabrication, low expense and high performance are indispensable for smart electronic integration [22–29]. Accordingly, design optimization on the structure and electronic system is a key approach to improve the output performance [30,31].

In this work, we demonstrated the robust design of unearthed single-electrode TENG (referred as h-TENG) made from copper foam and interlaced porous PDMS film (referred as CPDMS film). The as-fabricated one-chip h-TENG exhibits high mechanical durability, excellent stability and overall water resistance. Self-powered electrochromic device has also been explored by integration with PDLC (polymer dispersed liquid crystal), which can be utilized as intelligent

* Corresponding authors at: Beijing Institute of Nanoenergy and Nanosystems, Chinese Academy of Sciences, National Center for Nanoscience and Technology (NCNST), Beijing 100083, China; University of Science and Technology Beijing, Beijing 100069, PR China.
E-mail addresses: caoxia@binn.cas.cn (X. Cao), wangning@buaa.edu.cn (N. Wang), zlwang@gatech.edu (Z.L. Wang).

http://dx.doi.org/10.1016/j.nanoen.2016.10.002
Received 18 July 2016; Received in revised form 3 October 2016; Accepted 4 October 2016
Available online 04 October 2016

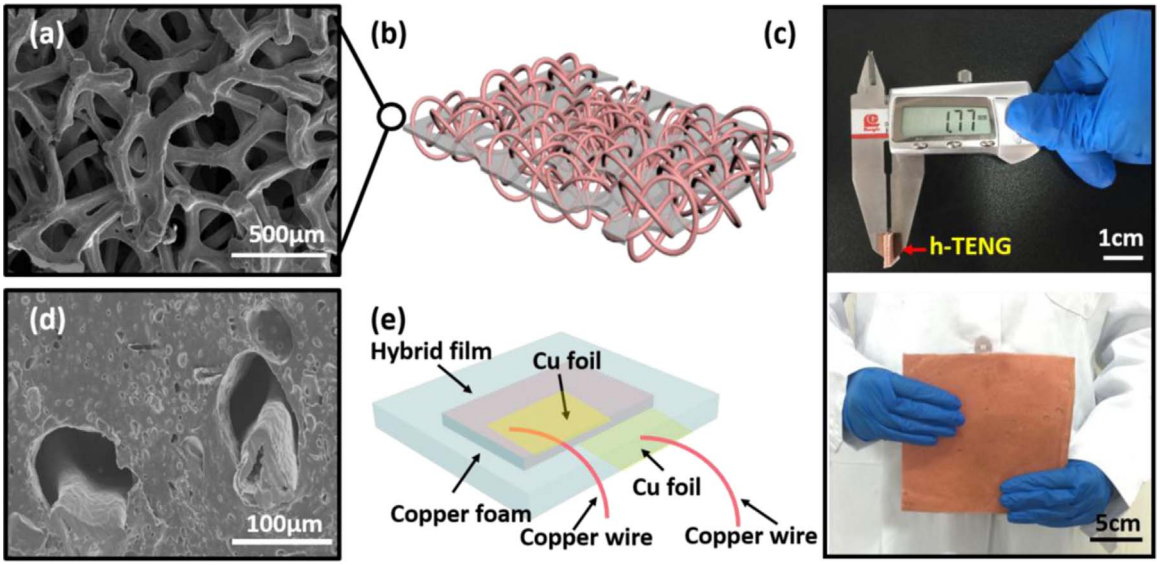

Fig. 1. (a, b) SEM image and the schematic diagram of the copper foam. (c) The as-fabricated h-TENGs with different sizes. (d) Cross-sectional SEM image of the hybrid film. (e) Schematic illustration of the h-TENG.

pressure sensors responding to tapping, pressing, treading and other mechanical movements.

2. Results and discussion

Morphology of the three-dimensional copper foam is shown in Fig. 1a, and the schematic diagram of the h-TENG is shown in Fig. 1b. After hybridization, the sponge-like three-dimensional pores are filled with PDMS film. Thickness of the h-TENG shown in Fig. 1c is of about 1.77 mm, which can be further tuned by changing the thickness of the copper foam. The cross-sectional view of the hybrid film demonstrates the micro gap between the copper foam and PDMS film because of the hydrophobicity (Fig. 1d). Scheme of the fabrication of the h-TENG is shown in Fig. 1e.

As shown by Fig. S1a, PDMS films prepared from mixed PDMS/water suspension is inclined to develop spherical pores along with the removal of the DI water because of the inherent hydrophobicity of PDMS. The powering Cu/PDMS films were prepared by the dip-coating method. It can be observed that PDMS infiltrates the copper foam and forms a sponge-like microstructure at this stage (Fig. S1a–d). Nevertheless, the conspicuous porosity in PDMS cannot be obtained without DI water (referred as PDMS-np, Fig. S1b), nor with acetone or methylene chloride (referred as PDMS-a/-m (Fig. S1c and d)). The boiling point of acetone and dichloromethane is much lower in comparison with water. It may be deduced that the organic solvents evaporate too fast to form the micro voids during the curing of PDMS. In contrast, the moderate evaporation rate of water is beneficial to the formation of micro pores in the curing process, and water can act as effective pore-making agent in large batch.

The electric properties of the h-TENGs are shown in Fig. 2. The short-circuit output current and the open-circuit output voltage are all measured under an acceleration of 3 m s^{-2}, a running distance of 63 mm and an external force of 15 N by a linear motor. It can be seen that the hybrid film prepared with 50% wt DI water shows a much higher current output than the pure PDMS (Fig. 2a and b), and the output current reaches 1.2 μA cm^{-2} even a pressure as small as 5 N cm^{-2} is applied (Fig. 2a). The voltage characterizations show a similar trend as that of the current. As shown in Fig. 2c and d, the open-circuit voltage of PDMS-p-based h-TENGs is much higher than that from the PDMS-np samples. It can be deduced the porous structure increases the contact surface and obviously enhances the output power of the h-TENG. In another test, film thickness doesn't show any obvious impact on output current of the h-TENG, as shown by Fig. 2e. Thus the film thickness is kept as 1.73 mm in this work. In Fig. 2f, PDMS-a/-d/-n based h-TENGs show approximate short-circuit output currents, according with the observation that neither acetone nor methylene chloride can endow the composite material with conspicuous porosity due to their fast evaporation speed.

The ductility and soundness were tested by a linear motor with an acceleration of 3 m s^{-2}, a running distance of 63 mm and an external force of 15 N. A steady output can be obtained from the h-TENG even after thousands of bending (> 2000 cycle, > 50°), demonstrating its good flexibility and fatigue-resistance property (Fig. S2a and b). In comparison with traditional TENGs, this porous h-TENG needn't to attach any metal electrode and can work in conditions of high humidity due to the excellent surface hydrophobic property. This feature distinguished itself sharply from the traditional TENGs because the attached metal electrode for the latter is sensitive to moisture. In the water-resistance experiment, the h-TENG was soaked with DI water for several hours. The output current (Fig. S2c) and the output voltage (Fig. S2d) are almost unchanged soon after it was taken out, demonstrating excellent water tolerance.

The most possible charge induction mechanism within the PDMS-p-based h-TENG is schematically shown in Fig. 3. Charges are resulted from the coupling of triboelectric effect and electrostatic induction, as demonstrated by the controlled experiments [3,30–34]. Here the interfacial charge dissipation model should be applied. Microscopically, when the h-TENG is squeezed, the copper foam and PDMS contact fully and friction occurs. Electrons are transferred from copper foam to PDMS film, resulting in positive charges on copper foam and negative charges inside the pores of PDMS at the squeezed spot. As the force is withdrawn, the copper foam is partly separated from PDMS film. On the other hand, we can always assume that the hybrid is uniform macroscopically though the elastic deformation caused by applied stress is always asymmetric, which decreases sharply along with the distance from the pressure point. Thus statically, PDMS film at the force point is apt to be negative charge while positive charges are always transported to bottom surface (assuming the force point as the upper surface) regardless the position of the copper foam within the pores. Under short-circuit condition, electrons near the squeezing spot move to far-end/bottom surface through an external circuit to neutralize the positive triboelectric charges, reaching an

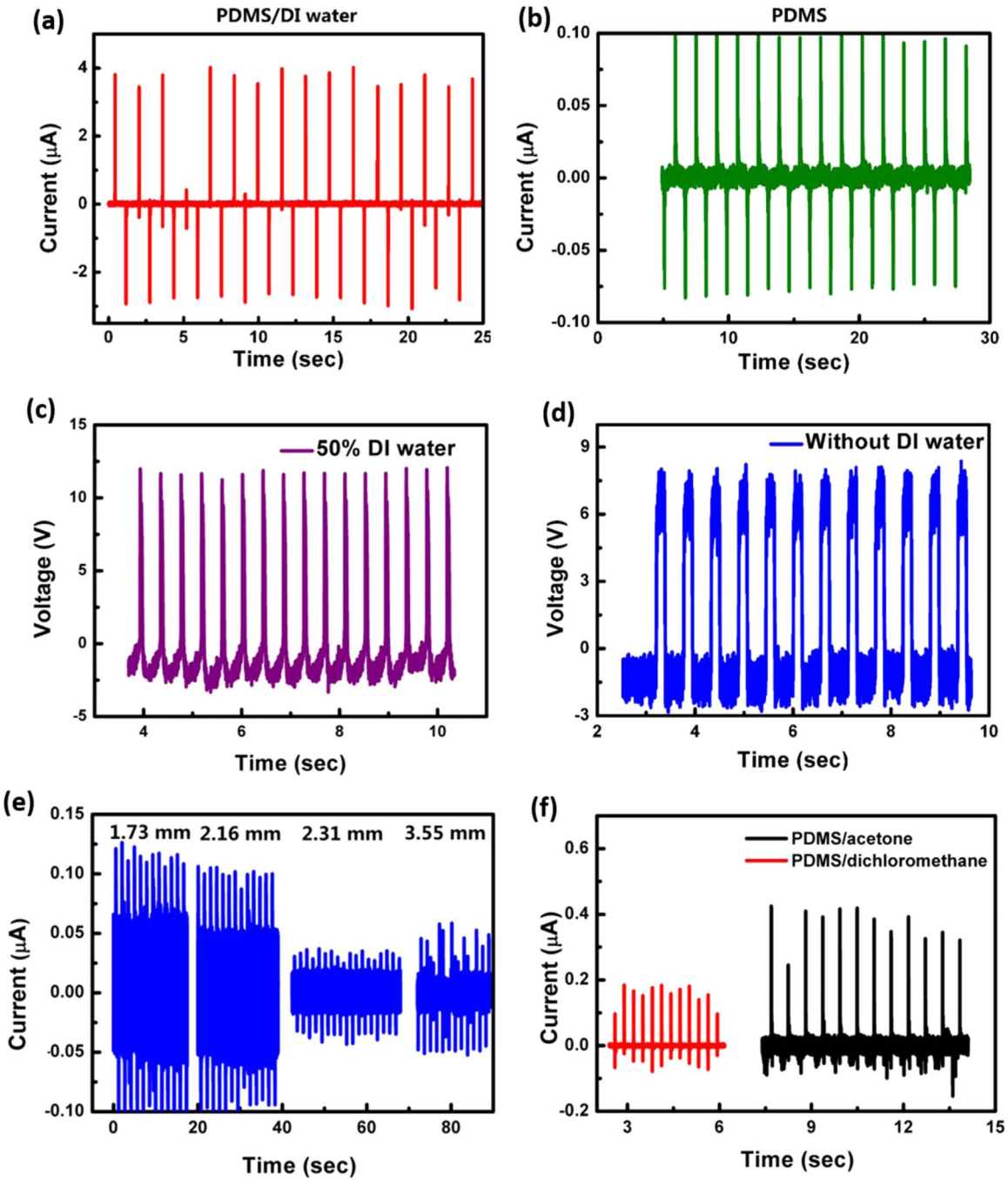

Fig. 2. Output current of the h-TENGs prepared with (a) and without DI water (b). (c, d) Corresponding voltages of the h-TENG prepared with 50% /without DI water. (e) Output currents of h-TENGs with different thickness. (f) Output currents of PDMS-a/PDMS-d based h-TENGs. The area of the as-prepared samples is 1 cm×3 cm.

electrostatic equilibrium and generating a negative current signal. When the hybrid electrode fully reverts to the initial position, there is no electron flowing through the circuit till the h-TENG is pressed again. In this circle, the copper foam will contact with PDMS again, causing the charges to disappear, and charges decrease on both of the top and bottom surface, which produces a downwards current. Therefore, electrons are driven from the non-contact pot/bottom layer back to contact spot/top layer, decreasing the amount of induced charges and leading to a positive current signal. At the end of the circle, copper foam and the PDMS inside the pores are in contact again and all induced charges are neutralized.

Meanwhile, the single-wire transmission mode also contributes to the charge generation at the skin-hybrid film interface (Fig. 4). Here once a relative separation between Cu electrode and skin occurs, negative charges on the surface of the skin induce positive charges on the Cu electrode, driving free electrons flowing from the far-end of the wire via the load (e.g., LEDs) to the Cu electrode (Fig. 4a–c). When negative triboelectric charges on the skin are fully screened from the induced positive charges on the Cu electrode by increasing the separation distance between the Cu and skin, no output signals can be observed, as illustrated by Fig. 4d. Besides, when the skin was reverted to approach the Cu electrode, the induced positive charges on the Cu electrode increase and the positive charges in the wire will flow from the far end of the wire to the Cu electrode until the skin and Cu fully contact with each other again, resulting in a reversed output voltage/current signal (Fig. 4e). This is another full cycle of the

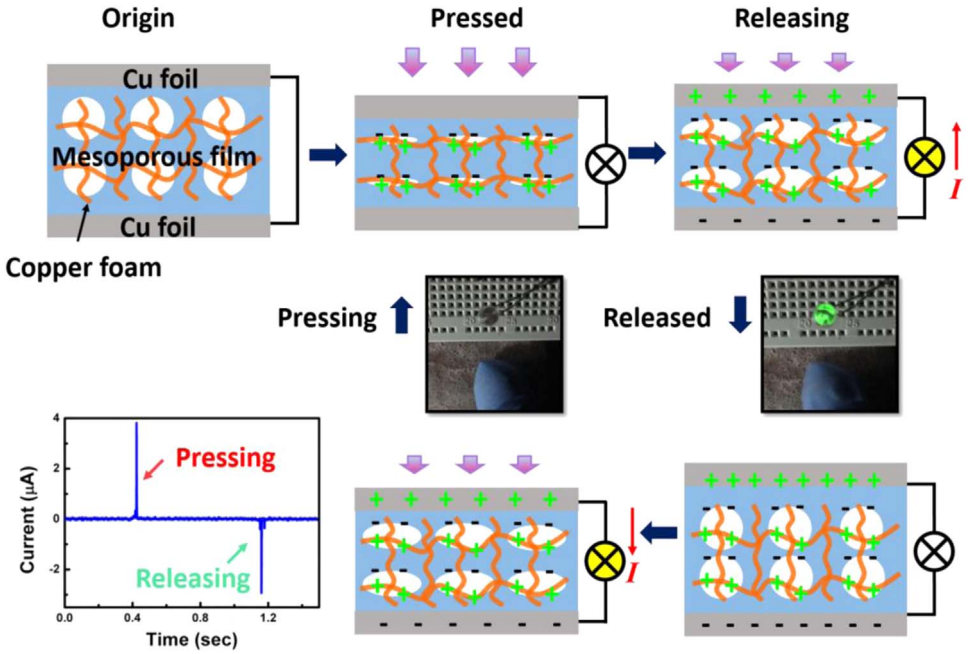

Fig. 3. Asymmetric deformation caused charge generation mechanism of the Cu-PDMS-based h-TENG.

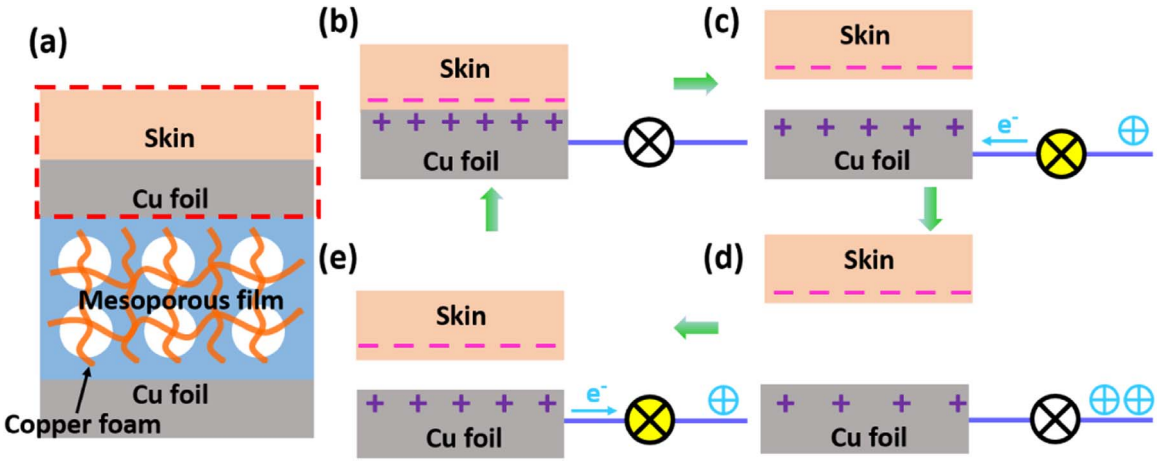

Fig. 4. Charge generation mechanism of the single-wire TENG without ground lead. (a) Structure of the device, (b–e) the working cycle of the TENG.

electricity generation process for this unearthed single-electrode TENG similar with the traditional contact-separation mode.

Recently, it has been demonstrated that single-electrode-based TENG with ground lead is also very useful for applications such as in displacement vector sensor system [35]. For example, when an object (such as glove, hand or foot) contacts with a copper film, triboelectrification first occurs with the contact and separation mode between copper film and the object. Then equivalent negative and positive charges generate and separate rapidly on the friction layer and object surface owing to different triboelectric series when the object tends to leave away. As the object leaves away, positive charges will be induced on copper film. Thus electrons from the ground flow to the copper electrode because of potential difference between the electrode layer and the ground, resulting in an electrical current. Until the object is quite far away, an electrical equilibrium achieves and the electrons stop moving. As the object approaches the metal electrode again, electrons flow inversely from the copper electrode to ground in order to reach a charge balance. When the object contacts with the metal electrode, charge neutralization occurs immediately [3,14]. However, there is no attached copper electrode on the h-TENG in this work. At the original position, skin and PDMS contact fully with each other, and surface charge transfer takes place at the contact point due to triboelectrification. According to the triboelectric series, electrons were injected from skin to PDMS in the contact electrification process because the PDMS is more triboelectrically negative than skin (Fig. 5a). The negative charges then induce the positive charge accumulation in Cu foam and its neighboring PDMS film due to the sound conductivity of copper (Fig. 5b). Until the skin is quite far away, an electrical equilibrium achieves and the electrons stop moving (Fig. 5c). Once the generator is pressed again, the induced positive charges on the Cu surface decrease. As a consequence, electrons are driven from the far-end/bottom surface back to the top surface, increasing the amount of induced charges (Fig. 5d). However, the charges on the PDMS surface belong to bound charge and it is non-ohmic contacts between PDMS film and copper wire, thus the contribution of this part to the overall output needs further consideration.

The h-TENG also enables fast switch of opaque-transparent and transparent-opaque states of the PDLC film by mechanical actions. The

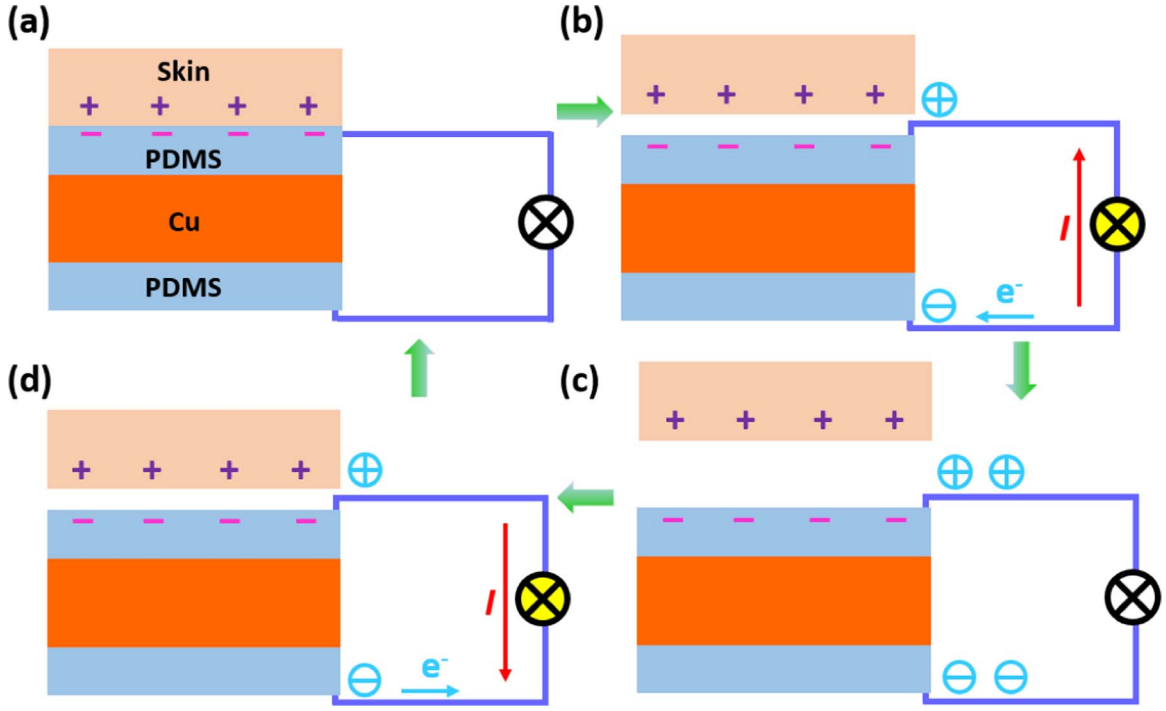

Fig. 5. (a–d) Electrostatically induced charge generation mechanism at the skin-h-TENG interface without attached electrodes. This is another configuration that we found that can generate electricity in practice.

working mechanism of the PDLC film is depicted by Fig. 6a. In the absence of any electric field, liquid crystal molecules are disorderly arranged, showing the opaque state. On the contrary, liquid crystal molecules in the PDLC film are arranged along the electric field direction and leads to the transparency of the PDLC film when energized. In this work, one piece of PDLC film was pasted onto the h-TENG surface to test its color change with an external pressure. As shown in Fig. 6b and c, the PDLC film becomes transparent and the bottom object appears from the PDLC film when a slight pressure is applied. As mentioned above, when a pressure is applied, an electric field will be generated on the h-TENG owing to coupled inductive effect, making the PDLC film energized and showing the trace of the pressure temporally. When the pressure disappears, the electric field is absent, and the trace is gone. The handwritten path on the PDLC film can then be captured in real-time for secure electronic signature collections (Fig. 6d and e). In the kinetic energy harvesting test, over thirty LED bulbs were lighten up upon slightly flapping the h-TENG (Fig. 6f and g). In this energy conversion process, the mechanical motion is not necessarily to be flat. It means that the h-TENG can be installed to the court, the plaza and even the subway as a stable power supply.

3. Conclusion

In conclusion, a simple strategy for fabricating unearthed single-electrode h-TENGs from hybrid Cu-PDMS films has been demonstrated. The as-fabricated single-electrode h-TENGs are not only stable and waterproof, but also sensitive to vibration and pressure and can be integrated into electrochromic devices for recording pressure trace. Thus this robust design represents a multifunctional platform for both energy harvesting and tribophototronics and can be used for interactive display, integrated circuits, and flexible/touch optoelectronics.

4. Experimental section

The PDMS monomers and curing agent was mixed in a mass ratio of 10:1 in a beaker. Deionized water (DI water) was then added to increase the porosity. In a typical process flow, the copper foam was first cleaned in an aqueous 1.0 M HCl solution for about 20 s, rinsed with DI water, then dried under a N_2 gas flow. In the controlled experiment, DI water was replaced by acetone and methylene chloride to tune the porosity of the film. Then the mixture was stirred for about 30 min and kept in a vacuum chamber to remove the air remained in PDMS. To prepare the hybrid film, the copper foam was dipped into the PDMS suspension for three hours. Thickness of the films can be controlled by repeating the dipping process. The hybrid CPDMS film was then placed on a SiO_2/Si mold and solidified in atmosphere at 90 °C for 1 h. The dried CPDMS film was peeled off from the substrate, thus a porous film was obtained.

The surface morphologies of the as-fabricated CPDMS film were characterized by a SU8020 field emission scanning electron microscope (SEM). The output voltage and current of the h-TENG were measured by applying an external force with a commercial linear mechanical motor (Linmot Inc.). The reciprocating motion of the generator was tuned by the motor-controlling program. The friction between the PDMS film and the copper foam resulted in a triboelectric potential and an electrical output in the external circuit. A Keithley Model 6514 System Electrometer was used to measure the open-circuit voltage, while we used an SR570 low-noise current amplifier (Stanford Research System) to measure the short circuit current.

Acknowledgements

We acknowledge financial support from the National Natural Science Foundation of China (NSFC Nos. 21275102, 21173017, 51272011 and 21575009), the Science and Technology Research Projects from Education Ministry (213002A), National “Twelfth Five-Year” Plan for Science & Technology Support (No. 2013BAK12B06), the “Thousands Talents” Program for Pioneer Researcher and His Innovation Team, China, and the National Natural Science Foundation of China (Grant Nos. 51432005 and Y4YR011001).

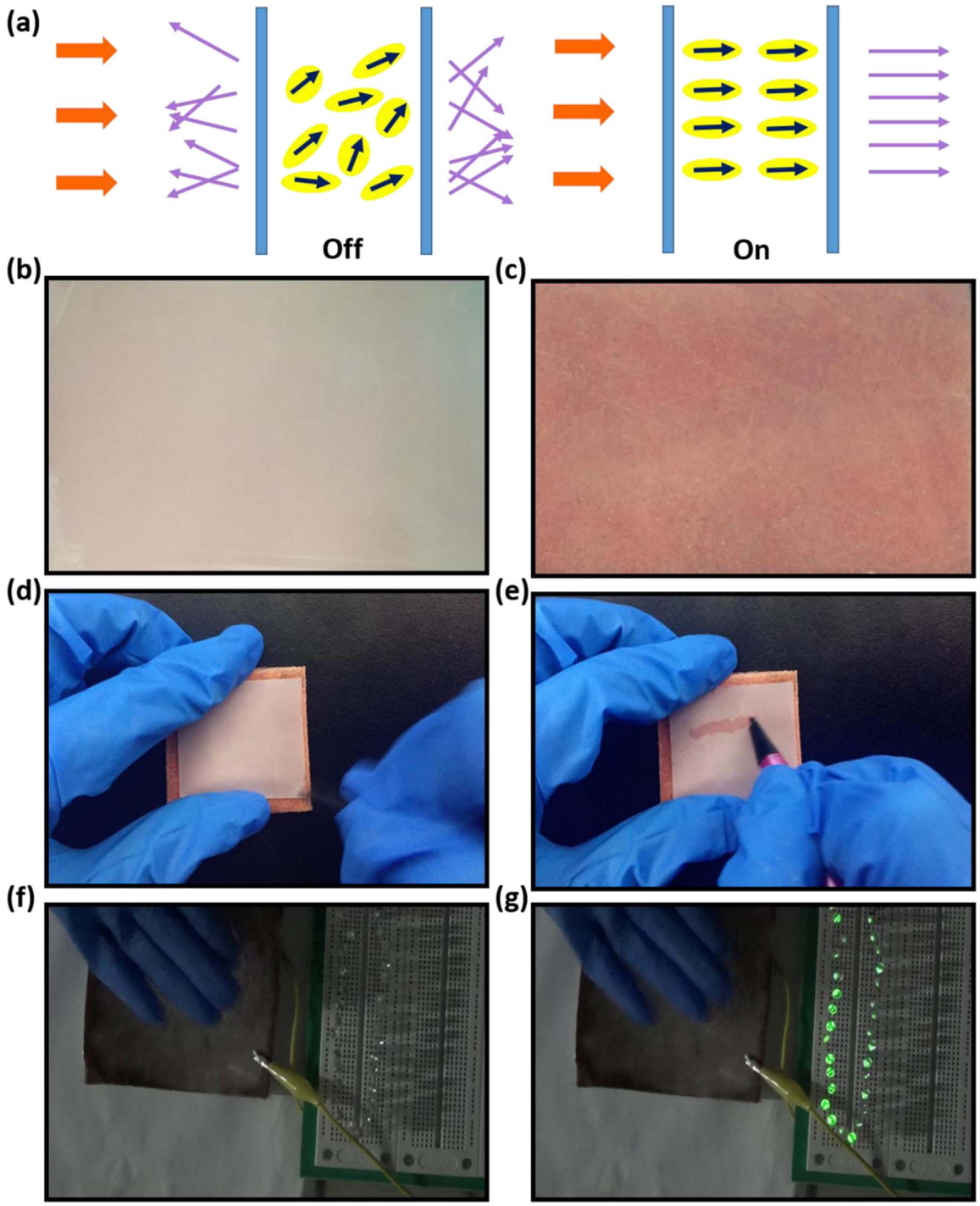

Fig. 6. (a) Working principle of the PDLC film. (b, c) Comparison of the non-energized/ energized states of the PDLC film. (d, e) Electrochromic trace catching. (f, g) Demonstration of integrated h-TENG in powering over 30 LED bulbs by harnessing hand flapping.

Appendix A. Supporting information

Supplementary data associated with this article can be found in the online version at doi:10.1016/j.nanoen.2016.10.002.

References

[1] Y. Liang, Z. Tao, J. Chen, Adv. Energy Mater. 2 (2012) 742–769.
[2] S.-W. Kim, D.-H. Seo, X. Ma, G. Ceder, K. Kang, Adv. Energy Mater. 2 (2012) 710–721.
[3] Z.L. Wang, ACS Nano 7 (2013) 9533–9557.
[4] S. Wang, Y. Xie, S. Niu, L. Lin, C. Liu, Y.S. Zhou, Z.L. Wang, Adv. Mater. 26 (2014) 6720–6728.
[5] W.U. Huynh, J.J. Dittmer, A.P. Alivisatos, Science 295 (2002) 2425–2427.
[6] G. Cheng, Z.H. Lin, L. Lin, Z.L. Du, Z.L. Wang, ACS Nano 7 (2013) 7383–7391.
[7] A. Wolfbrandt, IEEE Trans. Magn. 42 (2006) 1812–1819.
[8] X. Chen, M. Iwamoto, Z. Shi, L. Zhang, Z.L. Wang, Adv. Funct. Mater. 25 (2015) 739–747.
[9] S. Wang, L. Lin, Z.L. Wang, Nano Lett. 12 (2012) 6339–6346.
[10] Y. Su, X. Wen, G. Zhu, J. Yang, J. Chen, P. Bai, Z. Wu, Y. Jiang, Z. Lin Wang, Nano Energy 9 (2014) 186–195.
[11] G. Zhu, C. Pan, W. Guo, C.Y. Chen, Y. Zhou, R. Yu, Z.L. Wang, Nano Lett. 12 (2012) 4960–4965.
[12] F.R. Fan, L. Lin, G. Zhu, W. Wu, R. Zhang, Z.L. Wang, Nano Lett. 12 (2012) 3109–3114.
[13] Y. Jie, N. Wang, X. Cao, Y. Xu, T. Li, X.J. Zhang, Z.L. Wang, ACS Nano 9 (2015) 8376–8383.

[14] R.M. Yu, C.F. Pan, J. Chen, G. Zhu, Z.L. Wang, Adv. Funct. Mater. 23 (2013) 5868–5874.
[15] F.R. Fan, Z.Q. Tian, Z.L. Wang, Nano Energy 1 (2012) 328–334.
[16] Z. Li, J. Chen, J. Zhou, L. Zheng, K.C. Pradel, X. Fan, H. Guo, Z. Wen, M.-H. Yeh, C. Yu, Z.L. Wang, Nano Energy 22 (2016) 548–557.
[17] Y. Fang, J. Tong, Q. Zhong, Q. Chen, J. Zhou, Q. Luo, Y. Zhou, Z. Wang, B. Hu, Nano Energy 16 (2015) 301–309.
[18] X. Zhong, Y. Yang, X. Wang, Z.L. Wang, Nano Energy 13 (2015) 771–780.
[19] Z. Wen, J. Chen, M.-H. Yeh, H. Guo, Z. Li, X. Fan, T. Zhang, L. Zhu, Z.L. Wang, Nano Energy 16 (2015) 38–46.
[20] A.F. Yu, Y. Zhao, P. Jiang, Z.L. Wang, Nanotechnology 24 (2013) 055501.
[21] S.M. Niu, S.H. Wang, L. Lin, Y. Liu, Y.S. Zhou, Y.F. Hu, Z.L. Wang, Energy Environ. Sci. 6 (2013) 3576–3588.
[22] Z.H. Lin, Y.N. Xie, Y. Yang, S.H. Wang, G. Zhu, Z.L. Wang, ACS Nano 7 (2013) 4554–4560.
[23] Z.H. Lin, G. Zhu, Y.S. Zhou, Y. Yang, P. Bai, J. Chen, Z.L. Wang, Angew. Chem. 52 (2013) 5065–5069.
[24] Z. Li, J. Chen, J. Yang, Y. Su, X. Fan, Y. Wu, C. Yu, Z.L. Wang, Energy Environ. Sci. 8 (2015) 887–896.
[25] Y.K. Pang, F. Xue, L.F. Wang, J. Chen, J.J. Luo, T. Jiang, C. Zhang, Z.L. Wang, Adv. Sci. 3 (2016) 1500419.
[26] Z.L. Wang, Faraday Discuss. 176 (2014) 447–458.
[27] C. Zhang, W. Tang, C.B. Han, F.R. Fan, Z.L. Wang, Adv. Mater. 26 (2014) 3580–3591.
[28] C. Zhang, T. Zhou, W. Tang, C.B. Han, L.M. Zhang, Z.L. Wang, Adv. Energy Mater. 4 (2014) 1301798.
[29] S. Kim, M.K. Gupta, K.Y. Lee, A. Sohn, T.Y. Kim, K.S. Shin, D. Kim, S.K. Kim, K.H. Lee, H.J. Shin, D.W. Kim, S.W. Kim, Adv. Mater. 26 (2014) 3918–3925.
[30] A. Cherkasov, J. Chem. Inf. Comput. Sci. 43 (2003) 2039–2047.
[31] Y.F. Hu, Y. Zhang, C. Xu, G. Zhu, Z.L. Wang, Nano Lett. 10 (2010) 5025–5031.
[32] Z.C. Quan, C.B. Han, T. Jiang, Z.L. Wang, Adv. Energy Mater. 6 (2016) 1501799.
[33] Y.L. Zi, J. Wang, S.H. Wang, S.M. Li, Z. Wen, H.Y. Guo, Z.L. Wang, Nat. Commun. 6 (2015) 8376–8383.
[34] Z.L. Wang, Adv. Mater. 24 (2012) 280–285.
[35] Y. Yang, H.L. Zhang, J. Chen, Q.S. Jing, Y.S. Zhou, X.N. Wen, Z.L. Wang, ACS Nano (2013) 7342–7351.

Meng Zhang obtained her B.C. in polymer material and engineering from Dalian University of Technology (2014). Now she is doing her master degree at the Beijing Institute of Nanoenergy and Nanosystems, Chinese Academic Science. Her current research mainly focuses on material design and synthesis, energy harvesting and fabrication of devices.

Yang Jie is currently a Ph.D. candidate of the Research Center for Bioengineering and Sensing Technology at the University of Science and Technology Beijing, and joint training at the Beijing Institute of Nanoenergy and Nanosystems, Chinese Academy of Sciences. His research interests include electrochemical sensors and self-powered micro-/nano-systems.

Xia Cao is currently a distinguished professor at University of Science and Technology Beijing, and a professor at Beijing Institute of Nanoenergy and Nanosystems, Chinese Academy of Sciences. Her main research interests focus on the energy materials, nanoelectroanalytical chemistry, self-powered nano-biosensors and piezoelectric sensors.

Bian Jie obtained her B.C. in Chemistry and Chemical Engineering from Liaocheng University (2015). Now she is doing her master degree at the Beijing University of Aeronautics and Astronautics. (BUAA) Her current research mainly focuses on modification of materials and energy harvesting.

Tao Li received his B.C. in Material Chemistry (2011) and M.S. in Material Physic and Chemistry (2014) from Lanzhou University. Now he is a Ph.D. student at the Beijing Institute of Nanoenergy and Nanosystem, Chinese Academic Science. His current research mainly focuses on energy harvesting and fabrication of nanodevices.

Ning Wang obtained his Ph.D. from Beijing University of Aeronautics and Astronautics (BUAA) in 2008. He is currently a Professor of School of Mathematics and Physics, University of Science and Technology Beijing. His research interest is to understand fundamental mechanisms underlying experimentally observed phenomena with specific focus on electrochemical interface.

Zhong Lin (Z.L) Wang received his Ph.D. from Arizona State University in physics. He now is the Hightower Chair in Materials Science and Engineering, Regents' Professor, Engineering Distinguished Professor and Director, Center for Nanostructure Characterization, at Georgia Tech. Dr. Wang has made original and innovative contributions to the synthesis, discovery, characterization and understanding of fundamental physical properties of oxide nanobelts and nanowires, as well as applications of nanowires in energy sciences, electronics, optoelectronics and biological science. His discovery and breakthroughs in developing nanogenerators established the principle and technological roadmap for harvesting mechanical energy from the environment and biological systems for powering a personal electronics. His research on self-powered nanosystems has inspired the worldwide effort in academia and industry for studying energy for micro-nano-systems, which is now a distinct disciplinary in energy research and future sensor networks. He coined and pioneered the field of piezotronics and piezophototronics by introducing piezoelectric potential gated charge transport process in fabricating new electronic and optoelectronic devices. Details can be found at: www.nanoscience.gatech.edu.